

Improper Integrals Calculations for Fourier Boundary Element Method

Jan Sikora¹, Krzysztof Polakowski², and Beata Pańczyk¹

¹Electrical Engineering and Computer Science Faculty
Lublin University of Technology, 20-618 Lublin 38A Nadbystrzycka str., Poland
sik59@wp.pl, b.panczyk@pollub.pl

²The Faculty of Electrical Engineering
Warsaw University of Technology, 00-661 Warszawa, Pl. Politechniki 1, Poland
Krzysztof.Polakowski@ee.pw.edu.pl

Abstract—This paper presents a method of regularization for the numerical calculation of improper integrals used in different formulations of Boundary Element Method (BEM). The main attention of the readers we would like to focus on Fourier Formulation of BEM. The singular integrals arise when for discretization the elements of a higher order than zero are used. Very often in the Diffusive Optical Tomography for infant head modeling, triangular or square curvilinear boundary elements of the second order are used [12,14], hence, our interest in the subject of effective and accurate calculation of singular integrals. Even for the classical formulation of BEM such a problem is extremely difficult [1]. Some authors believe that the practical application possesses only flat triangular boundary elements of zero-order, and although there is some truth in this statement, the elements of the second order show a significant advantage [10,12] in Diffusion Optical Tomography (DOT) for example.

This issue becomes even more interesting when we deal with the Galerkin BEM formulation offering the possibility of matrix of coefficients symmetrisation, which has fundamental importance for inverse problems. This matter becomes critical when we start to consider the Fourier BEM formulation, introduced by Duddeck [5]. His approach provides the possibility of a solution in the case which has no fundamental solution. The light propagation, which is described by the Boltzmann equation (see Arridge [2]) is such a case.

Currently and most commonly, the Boltzmann equation is approximated by the diffusion equation in strongly light scattering media [10]. In the author's opinion, the problem of numerical integration of improper integrals has not yet been fully exhausted in the classic and Galerkin BEM formulation but the Fourier BEM formulation still expects the proposals of the effective solutions. Such an offer we would like to present in this paper.

Index Terms—Boundary element method, Fourier BEM, Galerkin BEM, numerical integration of singular integrals.

I. INTRODUCTION

In the field of digital modeling, two methods are used at present: the Finite Element Method (FEM) and the Boundary Element Method (BEM). The latter is less common since there is much less the professional computer software that uses the BEM compared to FEM.

For a few decades rapid development of BEM can be observed [1,5-7,9-12,14,15] resulting in an increase in BEM's application over time to, among other things, electromagnetic, thermal, and optical analysis [1,5-7, 11]. Nevertheless, it is not easy to find ready-to-use BEM implementations. The situation becomes even more difficult if we try to find free open source software and worse still if we need specialized BEM software applicable, for example, to Diffusion Optical Tomography. One of the reasons why this state is maintained might be the complexity of integration (in particular singular integrals) which needs to be done using BEM calculations. Of course, this is not a problem which cannot be overcome [12,14,15]. The need for the BEM calculations software exists and is unquestionable, but it has been only insignificantly implemented (Table 1 [10]). The other software packages for Boundary Element Methods is listed in Table 1. It is worth to emphasize that this list by no means is no complete.

It appears that industrial and scientific groups would like to have a well-designed platform for BEM calculations which should be universal but at the same time have modularity that easily enables application [8,14,15]. Such a software is collected in Table 2.

The plan of this article is as follows. In Section I, review the foundations of boundary element methods and standard methods for integration of singular integrals

is presented. Section II is devoted to a presentation of the major features of numerical integration for Fourier Boundary Element Method (FBEM). Finally, in Section

III we discuss plans for further directions of our research.

Table 1: Commercial software implementing BEM [11,12]

Library (Programme)	Environment (Language)	Application
BEASY	Windows or Unix binaries	Construction engineering
Integrated Engineering Software	Windows only	Fields, wave, thermal analysis
GPBEST	Windows or Unix	Acoustics, thermal analysis
Concept analysis	Windows	Stress analysis

Table 2: Free software implementing BEM [8,14,15]

Library	Language	Distribution Conditions	Application
ABEM (by Kirkup)	Fortran	Commercial, open source	Acoustics, Laplace and Helmholtz problems
LibBem	C++	Semi-commercial	Laplace equation
BEMLIB (Pozrikidis)	Fortran	GPL	Laplace, Helmholtz equations and Stokes flow
BIEPACK	Fortran	free open source	Laplace equation
BEA	Fortran	Distributed with the book	Acoustics
MaiProgs [8]	Fortran	Copyright © 2007 Matthias Maischak. Designed by Free CSS Templates. All templates are licensed under the Creative Commons Attribution 3.0 license.	Galerkin BEM for Laplace, Helmholtz, Lamé and Stokes equations
HyENA (Hyperbolic and Elliptic Numerical Analysis [16])	C++	Provided under the GNU Lesser General Public License	Laplace, Helmholtz and Lamé equations in 2D and 3D using the Galerkin or collocation approaches
BETL (Boundary Element Template Library [Hiptmair and Kielhorn 2012]; Kielhorn 2012)	C++	BETL is free for academic use in research and teaching	Laplace, Helmholtz and Maxwell equations in 3D using the Galerkin approach
BEM++ [13]	C++ Phyton	Open-source	Laplace, Helmholtz and Maxwell problems in three space dimensions
BEMlab [3]	C++	Open-source	Laplace, Helmholtz and Maxwell problems in three space dimensions

A. Standard 3D boundary element method and numerical integration of singular integrals

Let's consider Poisson's equation in three-dimensional space:

$$\nabla^2 \Phi(\mathbf{r}) = b, \quad (1)$$

where Φ stands for the arbitrary potential function for temperature or electric potential.

On the surface of the volume under consideration, the Robin boundary conditions are imposed:

$$\frac{\partial \Phi(\mathbf{r})}{\partial n} = m_R \Phi(\mathbf{r}) + n_R, \quad (2)$$

where m_R and n_R are known coefficients for the Robin boundary condition [2].

The fundamental solution for 3D space is:

$$G(|\mathbf{r} - \mathbf{r}'|) = \frac{1}{4\pi R}, \quad (3)$$

where $R = |\mathbf{r} - \mathbf{r}'|$ is a distance between \mathbf{r} (the source

point) and \mathbf{r}' (the field point).

The integral form for the Eq. (1) is:

$$c(\mathbf{r})\Phi(\mathbf{r}) + \int_{\Gamma} \frac{\partial G(|\mathbf{r} - \mathbf{r}'|)}{\partial n} \Phi(\mathbf{r}') d\Gamma(\mathbf{r}') = \int_{\Gamma} G(|\mathbf{r} - \mathbf{r}'|) \frac{\partial \Phi(\mathbf{r}')}{\partial n} d\Gamma(\mathbf{r}') + \int_{\Omega} bG(|\mathbf{r} - \mathbf{r}'|) d\Omega(\mathbf{r}'). \quad (4)$$

When the distance between the source point and the element over which the integration is performed is sufficiently large relative to the element size, the standard Gauss-Legendre quadrature formula works efficiently. But when the distance tends to zero than integrals became singular and special integration strategy should be applied.

Let us consider Quadrilateral boundary elements. The strategy used for integration rectangular boundary elements is as follows: mapping them at first onto 2D curvilinear coordinates and then dividing them into two

or three triangles and subsequently onto the standardized square. The whole procedure is shown in Fig. 1.

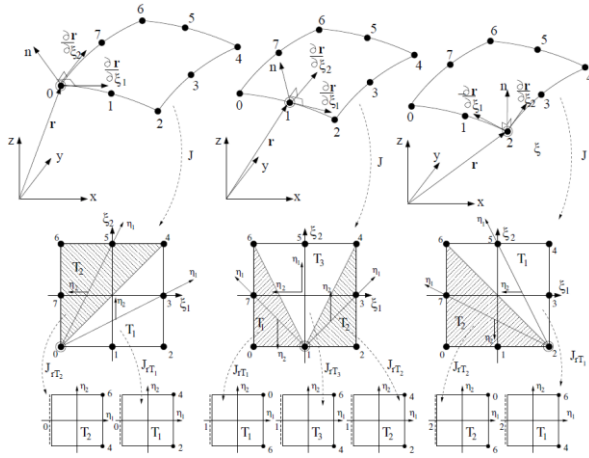


Fig. 1. Local coordinates of the quadrilateral boundary element and a mapping strategy [12].

Finally in all the above cases the Gauss – Legendre method of numerical integration was used [4]. The coordinates of the numerical integration points and the weights are available in the literature or in the internet, for example, [4,12].

II. FOURIER BOUNDARY ELEMENT METHOD (FBEM) AND NUMERICAL INTEGRATION

Let us briefly introduce some elements of basics of Fourier approach to BEM¹.

To obtain the Fourier transform of the Galerkin BEM, all quantities have to be extended from domain Ω to the space R^n . This can be achieved by defining a cutoff distribution χ [5], multiplying all quantities by χ and finally transforming the quantities into Fourier space:

$$F(u) = \hat{u}, \quad u \in L_1(R^n), \quad i = \sqrt{-1}.$$

The n -dimension Fourier transform is defined as:

$$\hat{u}(\hat{x}) = \int_{R^n} u(x) e^{-i\langle x, \hat{x} \rangle} dx, \quad (5)$$

$$\langle x, \hat{x} \rangle = \sum_{k=1}^n x_k \hat{x}_k. \quad (6)$$

The discretized Fourier BEM leads to an algebraic system identical to that obtained in the original space:

$$\sum_i K_u^{ji} u^i = F_u^j + \sum_i H_u^{ji} t^i - \sum_i G_u^{ji} u^i, \quad (7)$$

where now, the matrices and vectors are computed in the transformed space,

¹ Based on F.M.E. Duddeck. Fourier BEM. Springer-Verlag, 2002. Lecture Notes in Applied Mechanics, vol. 5.

$$\begin{aligned} F_u^j &= \frac{1}{(2\pi)^n} \langle \hat{\Phi}_t^j(-\hat{x}), \hat{f}(\hat{x}) \hat{U}(\hat{x}) \rangle, \\ G_u^{ji} &= \frac{1}{(2\pi)^n} \langle \hat{\Phi}_t^j(-\hat{x}), \hat{\Phi}_u^i(\hat{x}) \hat{A}_t^i \hat{U}(\hat{x}) \rangle, \\ H_u^{ji} &= \frac{1}{(2\pi)^n} \langle \hat{\Phi}_t^j(-\hat{x}), \hat{\Phi}_t^i(\hat{x}) \hat{U}(\hat{x}) \rangle, \\ K_u^{ji} &= \frac{1}{(2\pi)^n} \langle \hat{\Phi}_t^j(-\hat{x}), \hat{p}_u^i(\hat{x}) \rangle. \end{aligned} \quad (8)$$

A. Numerical example

The Fourier formulation of BEM is only presented for the boundary integral equations limited to constant elements and 2D space. As the test example, the Dirichlet problem of the Poisson equation is considered: $\Delta u(x) = -f(x), \quad x \in \Omega, \quad u(x) = u_t = 0, \quad x \in \Gamma. \quad (9)$

The Dirichlet problem is solved in a quadratic two-dimensional domain $\Omega [0, 1] \times [0, 1]$. At the boundaries, $u=0$ is imposed. The interior is subjected to stationary heat source f . The boundary Γ is divided into 16 elements. In our case when the source function $f=1$ the exemplary entries are:

$$\begin{aligned} H^{12} &= \frac{1}{(2\pi)^2} \langle \hat{\Phi}_t^1(-\hat{x}), \hat{\Phi}_t^2(\hat{x}) \hat{U}(\hat{x}) \rangle = \\ &= \frac{1}{(2\pi)^2} \int_{R^2} \frac{[i(e^{i\hat{x}_1/4} - 1)] [i(e^{-i\hat{x}_1/2} - e^{-i\hat{x}_1/4})]}{-\hat{x}_1 \hat{x}_1 (-\hat{x}_1^2 - \hat{x}_2^2)} d\hat{x}_1 d\hat{x}_2, \quad (10) \\ F^1 &= \frac{1}{(2\pi)^2} \int_{R^2} \hat{\Phi}_t^2(-\hat{x}) \hat{U}(\hat{x}) d\hat{x} = \\ &= \frac{-1}{(2\pi)^2} \int_{R^2} \frac{[i(e^{i\hat{x}_1/4} - 1)]}{-\hat{x}_1 (-\hat{x}_1^2 - \hat{x}_2^2)} d\hat{x}_1 d\hat{x}_2, \quad \text{for } f_0 = 1. \end{aligned}$$

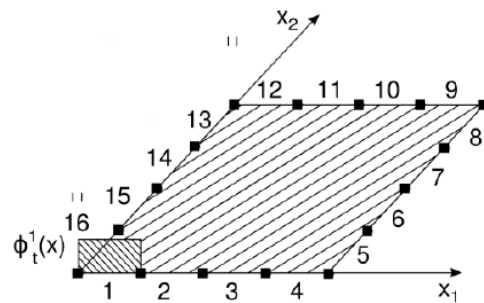


Fig. 2. Quadratic domain under consideration.

B. The integration in R^2 space and numerical challenges of improper integrals

Improper integrals present great challenges for numerical integration, but they are important in certain parts of science, like for example physics [13,14].

The trapezoidal and Simpson's methods use the value of the integrand at the endpoints of the domain of

integration. If the function is not defined there, these methods cannot be used. The midpoint and Gauss-Legendre methods use only interior points, so these are better suited to improper integrals.

However, as we will see, that these methods always return a result is not necessarily a good thing. Interior point methods return finite values when applied to both convergent and divergent integrals. It is something of an art to decide when an integral is divergent or how accurately the numerical value returned matches the integral.

C. Changing from infinite domains to finite domains of integration

Process of numerical integration in such a case of R^2 space could be divided into several steps.

STEP No. 1

The integrand (see Eq. (10)) has a singularity along the axis of the coordinate system x_1, x_2 as it is shown in Fig. 3. Therefore, in order to successfully integrate such a function numerically, we divide the space R^2 into four quarter in accordance with Fig. 4.

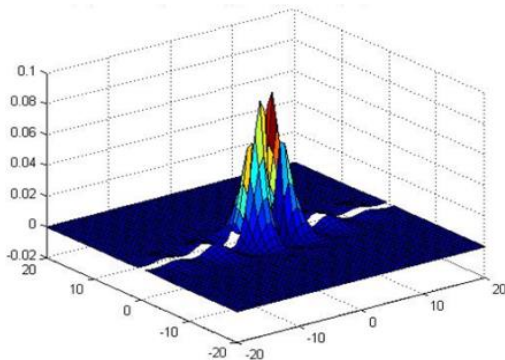


Fig. 3. Function being integrated in R^2 according to Eq. (10).

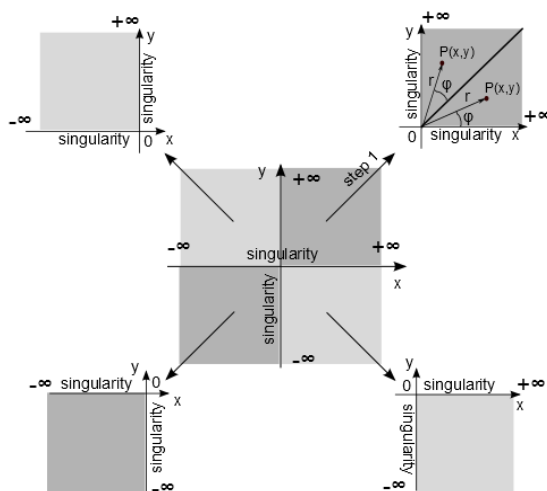


Fig. 4. R^2 space partition onto four quarters.

STEP No. 2

After dividing the area into four infinite subareas and unifying the limits of integration (for easier algorithmization) we have:

$$\int_{-\infty}^{\infty} \int_{-\infty}^{\infty} f(x_1, x_2) dx_1 dx_2 = \int_0^{\infty} \int_0^{\infty} f(x_1, x_2) dx_1 dx_2 + \int_0^{\infty} \int_{-\infty}^0 f(x_1, x_2) dx_1 dx_2 + \int_{-\infty}^0 \int_0^{\infty} f(x_1, x_2) dx_1 dx_2 + \int_{-\infty}^0 \int_{-\infty}^0 f(x_1, x_2) dx_1 dx_2 = \int_0^{\infty} \int_0^{\infty} f(x_1, x_2) dx_1 dx_2 + \int_0^{\infty} \int_0^{\infty} f(-x_1, x_2) dx_1 dx_2 + \int_0^{\infty} \int_0^{\infty} f(-x_1, -x_2) dx_1 dx_2 + \int_0^{\infty} \int_0^{\infty} f(x_1, -x_2) dx_1 dx_2. \tag{11}$$

After dividing the area into four infinite subareas and unifying the limits of integration, for easier algorithmization according to the last row of Eq. (11).

Every subarea was transformed into a local coordinate system using the transformation T (the same for both x_1 and x_2 coordinates):

$$x_i(\xi_i) = \frac{2\xi_i}{(1-\xi_i)^2}, \quad i = 1, 2, \tag{12}$$

where ξ_1, ξ_2 are the local coordinates.

Double integrals in local coordinates ξ_1, ξ_2 corresponds to the integration under square domain as it is shown in Fig. 5.

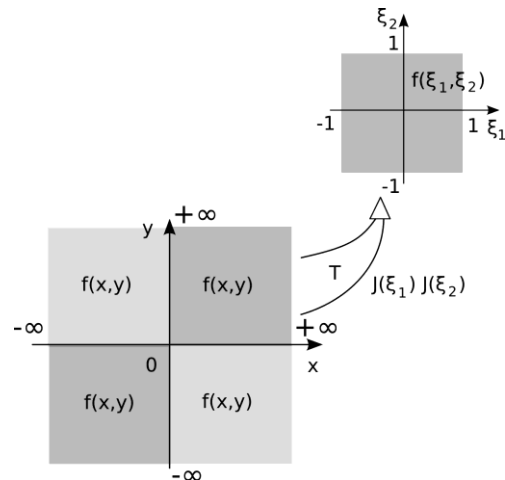


Fig. 5. One of the quarters after mapping into the normalized square.

The integrals can be calculated in a similar way as for the conventional BEM using twice Gauss-Legendre integration rules.

After transformation the numerical integration in the local coordinate system over each boundary element

is equal to:

$$I = \int_{-1}^1 \int_{-1}^1 f(x_1(\xi_1), x_2(\xi_2)) J(\xi_1) J(\xi_2) d\xi_1 d\xi_2, \quad (13)$$

where, f means any function for example the integrand from Eq. (10):

$$J(\xi_i) = \frac{dx_i}{d\xi_i} = \frac{2(1+\xi_i)^2}{(1-\xi_i^2)^2}, \quad i = 1, 2, \quad (14)$$

$J(\xi_i)$ for $i = 1, 2$, are the Jacobians of the transformation.

After transformation of one quarter of the integration space to the normalized square (see Fig. 5) the integrand from the Eq. 10 is presented in Fig. 6 (a). Unfortunately, we can observe a big oscillation close to the boundaries of the square. Oscillating functions are the most difficult for numerical integrations. That is why the 80 integration points were used (Fig. 6 (b)) to achieve satisfactory results.

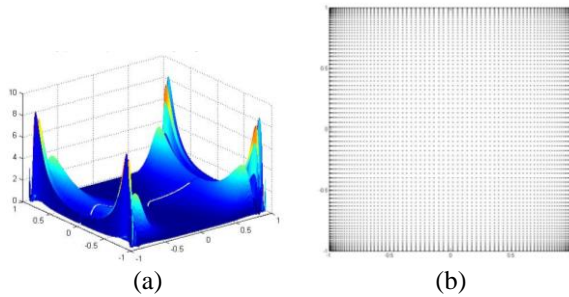


Fig. 6. (a) Function being integrated (see Eq. (10) after mapping into square. (b) For numerical calculation - the 80 integration points were used.

The 16 elements the coefficients matrix H (size of 4×4 , see Eq. 8) were calculated numerically and the results of calculations are shown in Table 3 for the region and its discretization shown in Fig. 2. As we can see the discretization is not particularly dense – only 16 elements. As a reference solution, the analytical integration was treated (see Table 3).

Table 3: Comparison between exact and numerical integration

Exact Solution	Numerical Solution	Relative Error [%]
0.166736	0.166059	0.41
0.336249	0.343520	2.16
0.336249	0.343520	2.16
0.166736	0.166059	0.41

In Fig. 7 the relative error of the final solution is presented.

One can say that the errors reported in the Table 3 are quite satisfactory. But still two problems remain. The first one that we are forced to use a vast number of

integration points what has a profound influence on the computation time for BEM. And the second problem that for the BEM such a level of relative error could not be sufficient in some applications like the DOT.

That is why we decided to develop the next steps of the integration procedure.

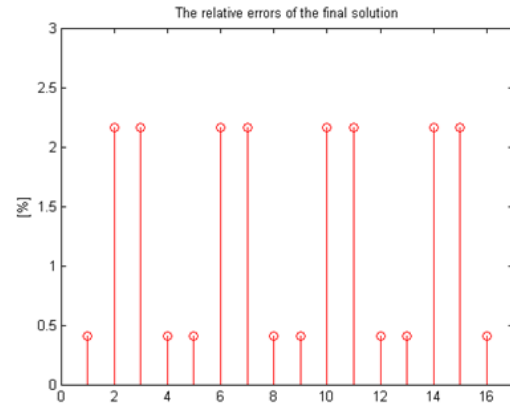


Fig.7. The relative error of the final solution.

STEP No. 3

Each quarter of the R^2 space is split onto two subspaces for which only one edge possess singularity as it is shown in Fig. 8.

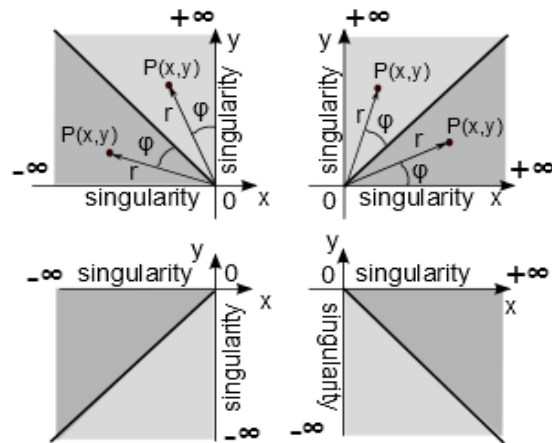


Fig. 8. Quarters are split onto eight parts.

STEP No. 4

Eight subspaces are mapped into the polar coordinate system. The polar coordinate system reduces infinity to one dimension only. In the Fig. 9 only the first two quarters of the R^2 space are presented but the rest is mapped in the similar way:

$$\begin{aligned} x(r, \Theta) &= r \cos \Theta, \\ y(r, \Theta) &= r \sin \Theta. \end{aligned} \quad (15)$$

Now, the Eq. (11) become more complicated as it is expressed in Eq. (16):

$$\begin{aligned}
 & \int_0^\infty \int_0^\infty f(x_1, x_2) dx_1 dx_2 + \int_0^\infty \int_0^\infty f(-x_1, x_2) dx_1 dx_2 + \\
 & \int_0^\infty \int_0^\infty f(-x_1, -x_2) dx_1 dx_2 + \int_0^\infty \int_0^\infty f(x_1, -x_2) dx_1 dx_2 = \\
 & \int_0^\infty \int_0^{\pi/4} f(r \cos \Theta, r \sin \Theta) r dr d\Theta + \\
 & \int_0^\infty \int_{\pi/4}^{\pi/2} f(r \cos \Theta, r \sin \Theta) r dr d\Theta + \\
 & \int_0^\infty \int_{\pi/2}^{3\pi/4} f(-r \cos \Theta, r \sin \Theta) r dr d\Theta + \\
 & \int_0^\infty \int_{3\pi/4}^\pi f(-r \cos \Theta, r \sin \Theta) r dr d\Theta + \\
 & \int_0^\infty \int_0^\pi f(-r \cos \Theta, -r \sin \Theta) r dr d\Theta + \\
 & \int_0^\infty \int_{\pi/4}^{\pi/2} f(-r \cos \Theta, -r \sin \Theta) r dr d\Theta + \\
 & \int_0^\infty \int_{3\pi/4}^{\pi/2} f(-r \cos \Theta, -r \sin \Theta) r dr d\Theta + \\
 & \int_0^\infty \int_{3\pi/4}^\pi f(r \cos \Theta, -r \sin \Theta) r dr d\Theta + \\
 & \int_0^\infty \int_{7\pi/4}^{2\pi} f(r \cos \Theta, -r \sin \Theta) r dr d\Theta .
 \end{aligned} \tag{16}$$

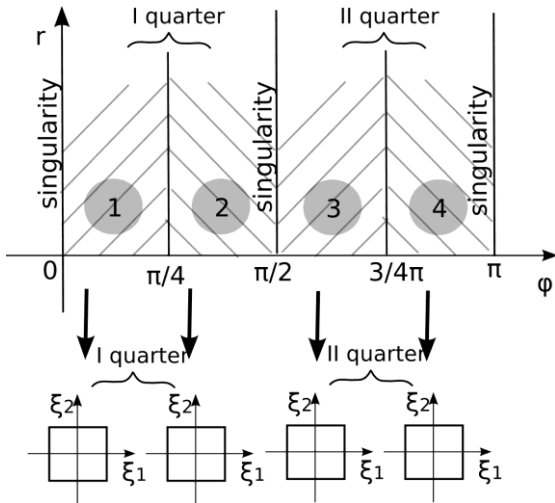


Fig. 9. The first two quarters are presented in polar coordinate system and next are mapped into normalized squares in local ξ_1, ξ_2 coordinate system.

STEP No. 5

Each of the eight subareas are transformed into a local coordinate system using the transformation T :

$$\begin{aligned}
 \Theta(\xi_1) &= \frac{\pi}{8} [\xi_1 + (2k-1)], \\
 r(\xi_2) &= \frac{2\xi_2}{(1-\xi_2)^2},
 \end{aligned} \tag{17}$$

where ξ_1, ξ_2 are the local coordinates, $k = 1 \div 8$ is the number of considered sub areas.

D. Using the Gauss-Legendre method of improper integrals with finite domains

After transformation, the numerical integration in the local coordinate system over each boundary element is equal to:

$$\begin{aligned}
 & \int_0^\infty \int_0^{\pi/4} f(r \cos \Theta, r \sin \Theta) r dr d\Theta = \\
 & \int_{-1}^1 \int_{-1}^1 f(r(\xi_2) \cos \Theta(\xi_1), r(\xi_2) \sin \Theta(\xi_1)) \\
 & r(\xi_2) J_\Theta(\xi_1) J_r(\xi_2) d\xi_1 d\xi_2,
 \end{aligned} \tag{18}$$

where, f means any function,

$$\begin{aligned}
 J_\Theta(\xi_1) &= \frac{d\Theta}{d\xi_1} = \frac{\pi}{8}, \\
 J_r(\xi_2) &= \frac{dr}{d\xi_2} = \frac{2(1+\xi_2)^2}{(1-\xi_2^2)^2},
 \end{aligned} \tag{19}$$

are the Jacobians of transformation and are the same for all eight subareas.

Next, we import the Gauss-Legendre coefficients from the following webpage:
http://www.math.ntnu.no/num/nmm/Program/Numlibc/gauss_co.c

III. CONCLUSION

This paper presents the regularization method for the integration of singular integrals for Fourier formulation of BEM. With the help of numerical experimentation, the effectiveness of the proposed method of integration was proven. Additionally, the authors tried to demonstrate that the degree of difficulty increases in the direction from the classical to the Fourier approach.

A very interesting formulation of the BEM was presented by Duddeck in his monograph [1], however the problem of integration was not considered thoroughly. One of the main goals of this paper was to address this gap. Without effective numerical integration, the Fourier approach to BEM becomes useless.

The authors believe that the Fourier's formulation holds enormous potential, for the Diffusion Optical Tomography. The light propagates in accordance with the Boltzmann equation [2]. The Boltzmann equation does not have a fundamental solution. Therefore, classical formulation of BEM becomes useless. Usually in case of environments strongly dissipative the Boltzmann equation is approximated by the diffusion equation [2,12].

The authors are aware that this work on numerical integration particularly in the R^2 space still required further work to improve the accuracy and reduce the number of integration points. This will be a critical

issue for real discretization with the aid of thousands of boundary elements.

ACKNOWLEDGMENT

This research was partially supported by the European Grant: OP VK 2.3. Elektrovýzkumník - reg.č. CZ.1.07/2.3.00/20.0175 - "Rozvoj potenciálu lidských zdrojů pro vědu a výzkum v oblasti elektrotechniky".

REFERENCES

- [1] M. H. Aliabadi and W. S. Hall, "The regularizing transformation integration method for boundary element kernels. Comparison with series expansion and weighted Gaussian integration methods," *Engineering Analysis with Boundary Elements*, vol. 6. No. 2, pp. 66-70, 1989.
- [2] S. R. Arridge, "Optical tomography in medical imaging," *Inverse Problems*, vol. 15, no. 2, pp. R41-R93, 1999.
- [3] BEMlab web page address: http://bemlab.org/wiki/Main_Page
- [4] C. Bond, "A new integration method providing the accuracy of Gauss-Legendre with error estimation capability." <http://www.crbond.com/papers/gbint.pdf>
- [5] F. M. E. Duddeck, *Fourier BEM*. Springer-Verlag, 2002. Lecture Notes in 258 Applied Mechanics, vol. 5.
- [6] T. Grzywacz, J. Sikora, and S. Wojtowicz, "Substructuring methods for 3-D BEM multilayered model for diffuse optical tomography problems," *IEEE Transactions on Magnetics*, vol. 44, no. 6, pp. 1374-1377, June 2008.
- [7] E. Łukasik, B. Pańczyk, and J. Sikora, "Calculation of the improper integrals for Fourier boundary element method," *Informatics Control Measurement in Economy and Environmental Protection (IAPGOS)*, ISBN 2083-0157, no. 3, pp. 7-10, 2013.
- [8] M. Maischak, Maiprogs, 2013. <http://www.ifam.uni-hannover.de/~maiprogs>
- [9] K. Polakowski, "Tomography visualization methods for monitoring gases in the automotive systems," Chapter in: *New Trends and Developments in Automotive Industry*, Edited by M. Chiaberge, (ISBN: 978-953-307-999-8), INTECH, pp. 193-208, 2011.
- [10] T. Rymarczyk, S. F. Filipowicz, J. Sikora, and K. Polakowski, "Applying the level set methods and the immersed interface method in EIT," *Electrical Review (PRZEGLĄD ELEKTROTECHNICZNY)*, R. 85, no. 4, pp. 68-70, 2009.
- [11] J. Sikora, A. Zacharopoulos, A. Douiri, M. Schweiger, L. Horesh, S. R. Arridge, and J. Ripoll, "Diffuse photon propagation in multilayered geometries," *Physics in Medicine and Biology*, vol. 51, pp. 497-516, 2006.
- [12] J. Sikora, *Boundary Element Method for Impedance and Optical Tomography*. Warsaw University of Technology Publisher, 2007.
- [13] W. Śmigaj, T. Betcke, S. R. Arridge, J. Phillips, and M. Schweiger, "Solving boundary integral problems with BEM++," *ACM Transactions on Mathematical Software*, vol. 41, no. 2, article 6, Publication date: January 2015, DOI: <http://dx.doi.org/10.1145/2590830>
- [14] P. Wieleba and J. Sikora, "Open source BEM library," *Advances in Engineering Software*, 2008, issn. 0965-9978, doi. 10.1016/j.advengsoft.2008.10.007.
- [15] P. Wieleba and J. Sikora, *BEMLAB – Universal, Open Source, Boundary Element Method Library Applied in Micro-Electro-Mechanical Systems*, Studies in Applied Electromagnetics and Mechanics 35, Electromagnetic Nondestructive Evaluation (XIV) Eds. T. Chady et. al., IOS Press, pp. 173-182, 2011.
- [16] <http://portal.tugraz.at/portal/page/portal/Files/i2610/files/Forschung/Software/HyENA/html/index.html>



Jan Sikora graduated from Warsaw University of Technology Faculty of Electrical Engineering. During 40 years of professional work he has proceeded all grades, including the position of Full Professor at his alma mater. Since 1998 he has worked for the Institute of Electrical

Engineering in Warsaw. In 2008 he has joined Electrical Engineering and Computer Science Faculty in Lublin University of Technology. His research interests are focused on numerical methods for electromagnetic field.



Krzysztof Polakowski graduated from Warsaw University of Technology Faculty of Electrical Engineering. During his studies, he has joined the Institute of Electrical Machines where he has achieved Ph.D. and defended Habilitatus work. His scientific interests are

concentrated on CAD method applied for numerical modelling in 3D space. Just recently his interests are focused on electromobility and industrial application of electrical tomography.



Beata Pańczyk graduated from mathematics at the Maria Curie-Skłodowska University in Lublin. Since 1989 she has been working at the Lublin University of Technology (LTU), where she completed a Ph.D. in 1996. The doctoral thesis title was “Construction of the Physical Properties Distribution Image using Impedance

Computer Tomography”. Currently she is the Senior Lecturer at the Institute of Computer Science of the LTU. Her didactic and research interest are: object oriented programming, web application development and application of numerical methods in engineering.